Nature Environment and Pollution Technology
An International Quarterly Scientific Journal
p-ISSN: 0972-6268
(Print copies up to 2016)
e-ISSN: 2395-3454
Vol. 24 No. 4 Article ID D1776 2025
Original Research Paper
https://doi.org/10.46488/NEPT.2025.v24i04.D1776
Open Access Journal

Superficial Urban Heat Island in the City of Santos, Brazil

Julio Angeles Suazo[1], Roberto Angeles Vasquez[2], Carmencita Lavado Meza[1], Nataly Angeles Suazo[3]†, Leonel de la Cruz Cerrón[4], Pabel Meza Mitma[1], Jose Flores Rojas[5] and Hugo Abi Karam[6]
[1]Universidad Nacional Autónoma de Tayacaja Daniel Hernández Morillo, Tayacaja, Perú
[2]Universidad Nacional del Centro del Perú, Huancayo, Perú
[3]Universidad Tecnológica del Perú, Lima, Perú
[4]Universidad Continental. Huancayo, Perú
[5]Instituto Geofísico del Perú. Lima, Perú
[6]Universidade Federal do Rio de Janeiro, Rio de Janeiro, Brazil
†Corresponding author: Nataly Angeles Suazo; nati2643@hotmail.com

Abbreviation: Nat. Env. & Poll. Technol.
Website: www.neptjournal.com

Received: 17-02-2025
Revised: 12-04-2025
Accepted: 16-04-2025

Key Words:

Urban heat island in Santos
Land surface temperature
Quantiles method
Streutker method
Urban-rural temperature contrast
Urban climatology

Citation for the Paper:

Angeles Suazo, J., Angeles Vasquez, R., Lavado Meza, C., Angeles Suazo, N., de la Cruz Cerrón, L., Meza Mitma, P., Flores Rojas, J. and Abi Karam, H., 2025. Superficial urban heat Island in the City of Santos/ Brazil. *Nature Environment and Pollution Technology*, 24(4), D1776. https://doi.org/10.46488/NEPT.2025.v24i04.D1776

Note: From 2025, the journal has adopted the use of Article IDs in citations instead of traditional consecutive page numbers. Each article is now given individual page ranges starting from page 1.

ABSTRACT

This contribution estimates the intensity of Urban Heat Island (UHI) during the period 2001 - 2020 for the city of Santos (CS), located in São Paulo, Brazil. The formation of the Surface Urban Heat Island (SUHI) was quantified from 2 methods: the first was Streutker's method, which adjusts the surface soil temperature (LST) (urban and rural surface) to a Gaussian surface. The second, the quantile method proposed by Jose Flores, uses the difference between the 0.95 quantile of the LST of the urban area and the median of the LST of the rural area. Both methods use remote sensing data of LST at 0.05° resolution, obtained from the MODIS sensor on board the TERRA and AQUA satellites. In general, the quantile method can be used as a complementary analysis to the Streutker method for cities with high LST. The results of the CS analysis, during diurnal periods, indicate maximum values in May (5.09°C) and minimum values in August (3.87°C). During the night period, it presented maximum values in February (3.94°C) and minimum values in August (2.40°C) with the quantile method, and due to its proximity to the Small Ocean, the Streutker method presents interferences.

INTRODUCTION

Urbanization produces significant changes in the radiative, thermal, and aerodynamic properties of surfaces through the formation of heat domes over cities, called urban heat islands (UHI) (Oke 1982, Arnfield 2003). The spatial distribution of UHIs is usually marked by a strong horizontal temperature gradient in the urban-rural boundary zone and a gradual decrease in temperature from the center to the edge of the city. These gradients are strongly affected by local circulation and climatic conditions; therefore, they are defined by diurnal and seasonal variations (Kim & Baik 2005, Roth 2007).

The main factors contributing to the formation and development of UHI spatial patterns include: scarcity of vegetation, extensive use of impervious surfaces, high thermal capacity, albedo of building materials and paving, which reduces evaporation, and this generates the typical three-dimensional geometry of urban surfaces (canyon-like configuration). For example, the existence of infrastructures with impermeable materials and thermal characteristics causes a decrease in albedo and an increase in surface temperature, as well as a reduction in relative humidity and evapotranspiration (Oke 1988, Kuang et al. 2017, Soltani & Sharifi 2017, Dai et al. 2019, Ouyang et al. 2022).

Industrial, human, construction, and transportation activities all contribute to the formation of heat islands, significantly affecting the local climate (Shahmohamadi et al. 2011, Wang et al. 2021). Since the urban surface traps the surrounding energy due to its extension, anthropogenic heat release also occurs through vehicle traffic, industrial/human processes, animal metabolism, and energy consumption, which generates a high rate of energy absorption due to the concentration of pollutants (gases and aerosols) in the urban atmosphere. In addition, the spatial patterns of UHI can be strongly influenced by the type of surface cover, such as green areas, water bodies and topography (Oke 1982, 1987, Kolokotroni et al. 2012). Some studies show that UHI can generate strong increases in surface temperature, low levels of specific humidity, and precipitation in urban coastal areas (Holst et al. 2016, Fung et al. 2021, Hu et al. 2021).

The present contribution proposes to estimate the SUHI of the city of Santos (CS) at low resolution during the period (2001-2020). The estimation is based on the use of the statistical quantile analysis method of LST data and the Streutker method, with low-resolution data obtained from the MODIS sensor on board the AQUA and TERRA satellites.

MATERIALS AND METHODS

The materials and methods are presented in three subsections: one describes where the measurements were made, another section describes the sensor used, and the last section describes the methods used for ICUS estimation.

Site and Location

The city of Santos (CS) is located in the southeast of South America, in Brazil, in the state of São Paulo. The state of São Paulo is composed of 39 municipalities (one of them called the municipality of Santos), with a total population of 20 million inhabitants, representing 11% of the population of Brazil, and has a relative humidity of 7% and annual accumulated rainfall of 400 mm (Flores et al. 2016).

To distinguish the behavior of LST throughout the year, both for urban and rural areas, and the relationship of these with vegetation cover, 3 points with different surface coverages were selected for the present study. Fig. 1a shows the rural location identified with (23.89 S, 46.20 W), Urban (23.95 S, 46.37 W), and border (23.94 S, 46.27 W), identified by the letters R, U and B, respectively.

MODIS Data

The MODIS sensor of the AQUA and TERRA satellites was used, where the MODIS thermal infrared (TIR) sensors measure radiances of the top of the atmosphere (TOA). These brightness temperatures are different from Land Surface Temperature (LST) with a difference of 1 to 5 K, due to the non-vertical satellite viewing angle, urban geometry, sub-pixel variation of surface temperature, variable surface emissivity, and various atmospheric effects (Dousset & Gourmelon 2003). In addition, MODIS AQUA has a better representation of LST/UHI, unlike other satellites (Zargari et al. 2024).

To remove these effects and estimate LST from space, a MODIS LST day-night method has been designed to take advantage of the unique capability of the MODIS instrument (Wan 1999). This method uses day-night pairs of TIR data in seven MODIS bands to simultaneously retrieve surface

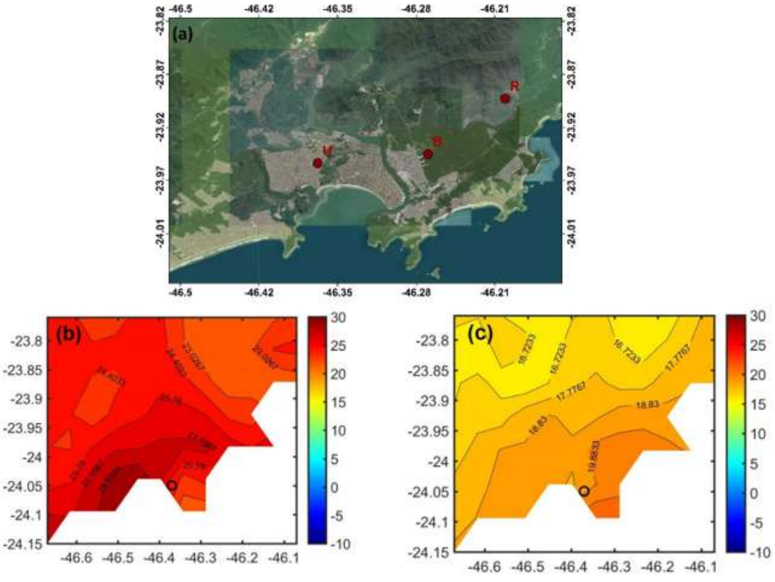

Fig. 1: (a) Area delimited as the CS domain, showing rural R (23.89 S, 46.20 W), Urban U (23.95 S, 46.37 W) and border B (23.94 S, 46.27 W), (b) monthly mean LST during the daytime period and (c) monthly mean LST of the nighttime period, both for December 2001.

temperatures and band-averaged emissivities in bands 20, 22 23, 23, 29, and 31-33 without knowing the water vapor and atmospheric temperature profiles with high accuracy (Wan & Li 1997). In addition, to generate more regionally representative urban temperature estimates, three-dimensional roughness of urban surfaces, which depends on satellite imagery, was considered (Voogt & Oke 2003).

In the present study, monthly averaging and scaling up to 5 km resolution were performed to analyze the effects of rescaling on the LST statistical patterns and then compared to the MOD11C3 Global CMG product, which is a composite monthly average derived from the MOD11C1 daily global product. These data are stored as clear-sky LST values over a period of months at a resolution of 0.05° (5600 meters).

To separate urban and rural areas, the MCD12C1 MODIS land cover product type MCD12C1 with 0.05° resolution was used to classify the land surface according to the International Geosphere-Biosphere Project (IGBP), 17 land cover types. In this categorization, an urban category has been obtained from MODIS version 4 observations following the contribution of Schneider (Schneider et al. 2003) (Fig. 2b).

SUHI Estimation

To determine the SUHI, the Gaussian Method (Streutker 2003) and the quantile method (Flores et al. 2016) were used; both methods were used in the estimation of urban surface heat island in the cities of Arequipa, Huancayo and Iquitos, e.g., Suazo et al. (2020).

The Streutker Method proposed by Streutker (2003) was used to determine the SUHI. The technique uses a least-square fit of the entire heat island to a Gaussian surface of the form:

$$T_{(x,y)} = T_0 + a_1 x + a_2 y + a_0 e^{\left(-\frac{(x-x_0)^2}{2a_x^2} - \frac{(y-y_0)^2}{2a_y^2}\right)} \quad ...(1)$$

Where $T_{(x,y)}$ is the total surface temperature, including urban and rural pixels. T_0, a_1 and a_2 are the constant and linear components of the rural temperature, respectively.

The quantile method proposed by Flores et al. (2016) to estimate the SUHI intensity is based on the statistical analysis of urban and rural LST quantiles. He also proposed the following formula to estimate the SUHI intensity for a resolution of 5 km:

$$SUHI = Q_5^{urban} - Q_3^{rural} \quad ...(2)$$

Where Q_5^{urban} is the 0.95 quantile of the LST distribution over the urban area and Q_3^{rural} Is the median of the LST distribution over the rural area, both with a resolution of 5 km.

RESULTS AND DISCUSSION

The results for the long-term (2001-2020) diurnal SUHI magnitudes and spatial extents for all months over the CS using the Streutker method are presented in Table 1. The highest SUHI intensity for the period occurred in November (3.19*°C*), and the lowest SUHI intensity was observed in

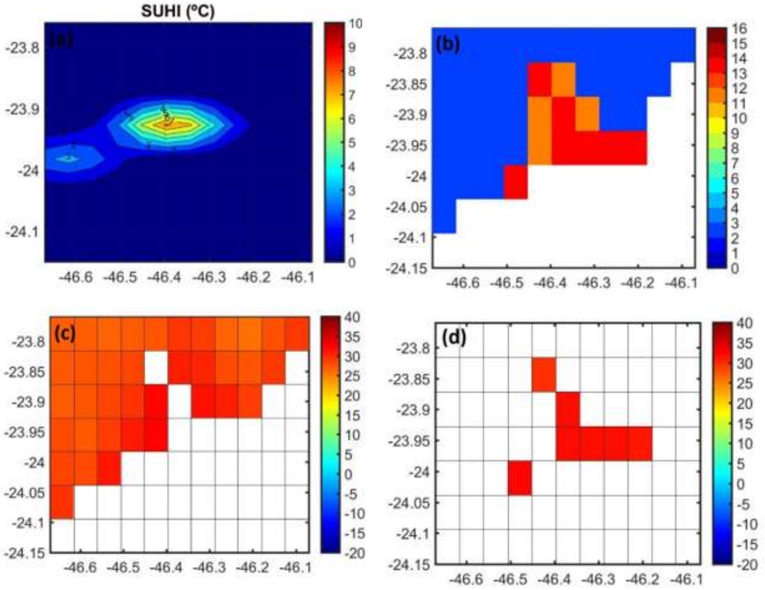

Fig. 2: (a) Least-Squares planar interpolation for rural LST, (b) Land cover type for December 2006 according to the IGBP, (c) Monthly mean diurnal LST (5km resolution) under the urban area of the MSA for January 2001, (d) Monthly mean diurnal LST of the rural area of the CS for January 2001.

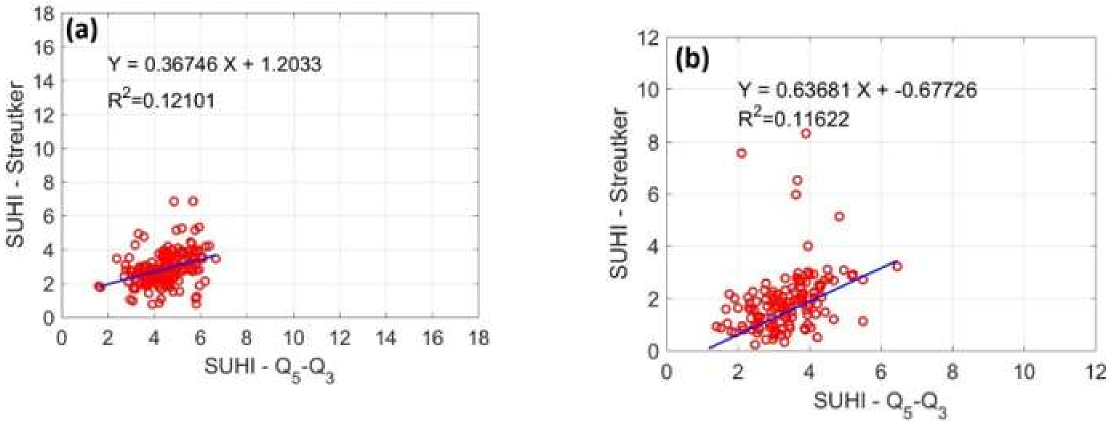

Fig. 3: (a) Scatter-plot of SUHI in diurnal periods, obtained with Streutker's method vs SUHI with the quantile difference Q_5^{urban} and Q_3^{rural} For the MSA, (b) nocturnal period.

January (2.62℃). On the contrary, for Suazo et al. (2019), the maximum values were found in September and the minimum in May. Heat stress, usually in the afternoon, limits daily vitality on the public highway (Soltani & Sharifi 2017). On the other hand, there is a correlation between the increase in vegetation and colder areas (Anees et al. 2025). Additionally, high temperatures predominate in the central region of the city and decrease as the distance from the city increases, being lower in the rural areas, as indicated by Novio et al. (2024).

Fig. 3a shows the scatter plot between the two methods for all months. The slope of the linear adjustment of the data is equal to 0.3, the intersection is at point 1.2, and the correlation found between both methods is equal to 0.12. Although they are calculating the same variable, they are not related in terms of their estimation. Likewise, in Fig. 3b for the night period, the linear fit to the data show a slope equal to 0.63, the intersection is equal to -0.67, and the correlation index is equal to 0.11. However, according to the research of Peng et al. (2024), there is an increasing trend of SUHI in areas with urban expansion during summer; moreover, there are decreasing ranges and intensities of SUHI in areas with high altitude and low economic level, while with high economic level and low altitude, there are cities with dominant increases. In addition, LST is negatively correlated with proximity to the coast during the day and positively correlated at night in SUHI studies (Jacobs et al. 2020, You et al. 2021, Chen et al. 2022).

For the CS, the results of the SUHI calculation using the statistical method of quantiles and Streutker in diurnal and nocturnal periods are shown in Table 1. The SUHI intensities with the diurnal quantile method present maximum values in May (5.09℃) and minimum values in August (3.87℃). SUHI intensities with the quantile method for the nocturnal period present maximum values in February (3.94℃) and minimum values in August (2.40℃). In general, the Streutker method underestimates the SUHI intensities; this characteristic is best observed during the night period, as demonstrated by Suazo et al. (2019). However, for Ma et al. (2024), they were lower values being 0.97 ± 0.78℃ and 0.21 ± 0.87℃ during the day and night, respectively, since at high altitudes, the nocturnal temperature is slightly higher than the diurnal, due to atmospheric pressure limiting heat reduction and conduction.

On the other hand, in the case of Zargari et al. (2024), higher values have been observed in the suburbs during the day, while at night, in central urban areas, for García (2022), cities near the coast have a higher diurnal temperature (SUHI = 1.44℃, LST = 3.90°C) and decreases as one moves away (SUHI = 0.52°C, LST = 2.85°C), and for Shapiro & Liu (2023), the LST values are higher in coastal areas, being the maximum 36.90°C and 33.55°C in the wet and dry season, respectively, but as it decreases at night. In the case of Wu et al. (2019), they mention that the distance to the coast does not influence the UHI effect, and the vegetation cover is more related to SUHI, both for spring and summer, in addition to the population density.

Furthermore, as mentioned by Hardin et al. (2018), surface characteristics are not the only factor influencing SUHI, as air pollution and meteorological conditions can affect variation, and it should be noted that LST has a relationship with N_2O levels (Suthar et al. 2023), therefore, there are higher values in spring in highly industrialized areas with little vegetation and excessive levels of nitrogen compounds (Kazemi et al. 2025) compared to green spaces (Feizizadeh & Blaschke 2013). Thus, there is a relationship between air pollutants and surface conditions with SUHIs (Iungman et al. 2024) and urban morphology (Esposito et al. 2024).

Table 1: Daytime and nighttime mean SUHI and spatial extent with standard deviation for the CS using the method developed by Streutker (2002) and Flores (2016) for the period 2001-2020.

Months	Suhi Streutker Daytime [℃]	Suhi Cuantil Daytime [℃]	Suhi Cuantil Night [℃]
January	2.62±1.66	4.67±0.76	3.59±0.99
February	2.91±0.81	4.96±0.86	3.94±0.82
March	2.79±0.85	4.26±0.83	3.60±1.10
April	3.05±0.55	4.77±0.79	3.56±0.64
May	3.01±0.69	5.09±0.53	3.32±0.55
Juny	2.52±0.57	4.03±0.73	2.69±0.81
July	2.73±0.59	4.02±0.57	2.44±0.56
August	2.71±0.48	3.87±0.64	2.40±0.46
September	3.05±1.18	4.05±1.09	2.71±0.60
October	3.01±0.84	4.38±1.24	3.46±1.09
November	3.19±1.19	4.74±1.07	3.89±0.53
December	2.31±1.28	3.91±0.99	3.69±0.85

The monthly behavior of the SUHI seen in Fig. 4a and 4b shows that, although the LST has a strong variation, the SUHI intensities and the monthly variation are little influenced in terms of amplitude, observed for both Streutker and quantile methods. During the night period, the mean rural LST drops significantly, which becomes m the quantile 0.95 (Q_5) of the urban area and the median (Q_3) of the rural area for the CS (Fig. 4b). The main causes that generate these differences between both methods may be the LST pattern over the rural area does not fit well in a straight plane because the pixel is close to Santa Rita lagoon and finally with the small Sea, these water bodies manage to retain large amounts of energy and influence the heat dispersion in the vicinity. An example is the case of Yao et al. (2018), when using nearby suburban areas as a reference background, an underestimation of SUHI of about 1.48°C is generated, while ignoring water bodies and elevation effects with rural area selection leads to an overestimation of SUHI by 1.63°C in 31 cities in China. In addition, as indicated by Du et al. (2025), the identification of LST grid anomalies (LSTA) can be used to decrease the bias by identifying LST anomalies in the grid (LSTA) to pinpoint the transition of urban areas. On the other hand, urban areas with higher building density and minimal vegetation cover are warmer by 1.2°C compared to environments with more open buildings, while natural areas are 2.4°C colder than areas with agglomerated buildings and 1.3°C colder with more open buildings (Suthar et al. 2023). In addition, there are soil indices such as NVDI, NDBI, and NDWI that provide a complement to the analysis by LST, to improve the compression of the temperature variation of the UHI (Nandi et al. 2024) and to consider the uncertainty generated

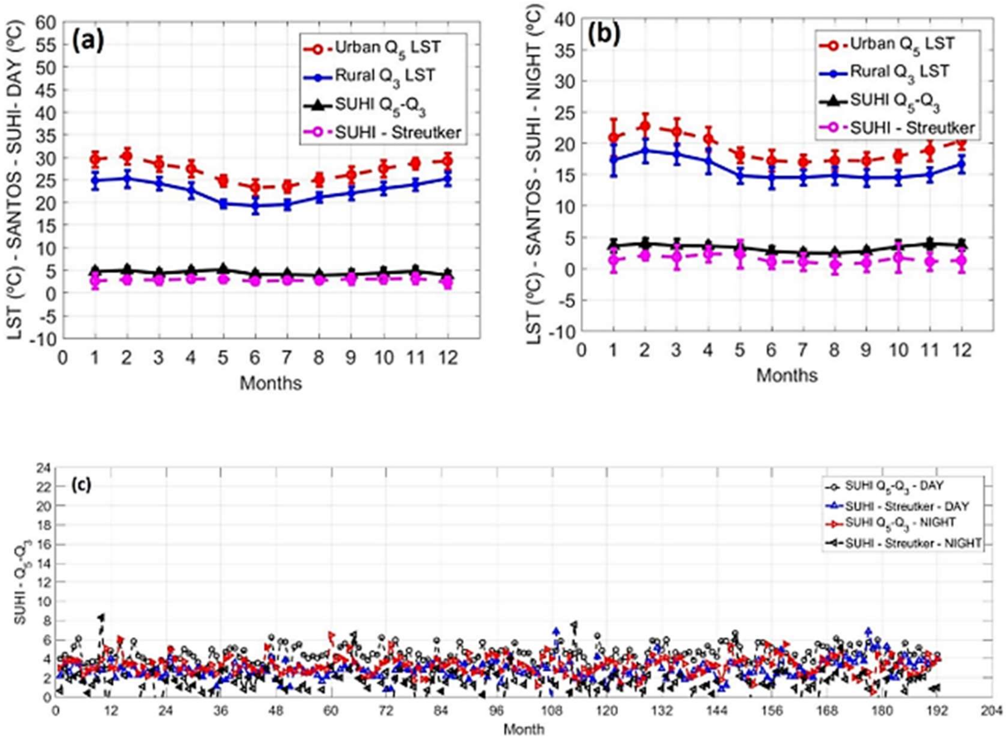

Fig. 4: (a) Time evolution from 2001-2020, monthly mean diurnal LST (°*C*) with standard deviation for diurnal period of urban LST (Q_5), rural LST (Q_3), SUHI intensity (°*C*) for CS, (b) night period. (c) Monthly evolution of SUHI by Streutker method and quantiles.

by estimating temperature through retrieval algorithms from satellite remote sensing (Hurduc et al. 2024).

In this work, as seen in Fig. 2a, there are two centers of maximum temperatures; thus, the cantile method was useful to perform the complementary analysis of the Streutker method due to the presence of more than one center of maximum surface temperature as suggested by Flores et al. (2016). Improving the understanding of heat island behavior can help in the formulation of new urban environmental policies and improved public life management focusing on climate change (Soltani & Sharifi 2017), towards more sustainable and climate-resilient cities in similar urban contexts (Anees et al. 2025). For example, according to Luo et al. (2025), a cooling network can be realized, connecting the heat island and cold island with a basis on circuit theory to organize cooling corridors and reduce SUHI intensity, towards climate resilient urban planning and organization.

CONCLUSIONS

With the help of the data obtained from the MODIS sensor, the main objective was to estimate the SUHI during the period (2001-2020) at a resolution (0.05°) for the CS, with the Streutker and quantile method, divided into 2 cases: urban and rural areas separated with the help of the Land Cover Type MODIS product. According to the analysis and evidence presented in this paper, it was concluded:

The methods used for SUHI estimation in the diurnal period present little correlation between them; these have a better fit during the nocturnal period. This could be explained by the existence of more than one center of maximum surface temperature during the day.

For the CS, during the diurnal periods, the SUHI intensity in May and August represents the maximum and minimum increase that could be reached within the urban area compared to rural areas. The nocturnal period presented maximum values in February and minimum values in August using the quantile method. In general, it was possible to show the formation of the heat island in the CS, with estimated increases greater than 5 $^{\circ}C$ during the day and close to 4 $^{\circ}C$ during the night. It is also recommended that future research use the MODIS sensor at higher spatial resolution and investigate urban planning strategies to mitigate the effects of heat islands.

ACKNOWLEDGMENTS

The surface temperature data sets were obtained from NASA from their website at http://modis.gsfc.nasa.gov/

REFERENCES

Anees, S.A., Mehmood, K., Raza, S.I.H., Pfautsch, S., Shah, M., Jamjareegulgarn, P., Shahzad, F., Alarfaj, A.A., Alharbi, S.A., Khan, W.R. and Dube, T., 2025. Spatiotemporal analysis of surface Urban Heat Island intensity and the role of vegetation in six major Pakistani cities. *Ecological Informatics*, 85, p. 102986. [DOI]

Arnfield, A.J., 2003. Two decades of urban climate research: A review of turbulence, exchanges of energy and water, and the urban heat island. *International Journal of Climatology*, 23(1), pp. 1–26. [DOI]

Chen, H., Deng, Q., Zhou, Z., Ren, Z. and Shan, X., 2022. Influence of land cover change on spatio-temporal distribution of urban heat island — a case in Wuhan main urban area. *Sustainable Cities and Society*, 79, p. 103715. [DOI]

Dai, Z., Guldmann, J.M. and Hu, Y., 2019. Thermal impacts of greenery, water, and impervious structures in Beijing's Olympic area: A spatial regression approach. *Ecological Indicators*, 97, pp. 77–88. [DOI]

Dousset, B. and Gourmelon, F., 2003. Satellite multi-sensor data analysis of urban surface temperatures and landcover. *ISPRS Journal of Photogrammetry and Remote Sensing*, 58, pp. 43–54. [DOI]

Du, Y., Xie, J., Xie, Z., Wang, N. and Zhang, L., 2025. Spatiotemporal footprints of surface urban heat islands in the urban agglomeration of Yangtze River Delta during 2000–2022. *Remote Sensing*, 17(5), p. 892. [DOI]

Esposito, A., Pappaccogli, G., Donateo, A., Salizzoni, P., Maffeis, G., Semeraro, T., Santiago, J.L. and Buccolieri, R., 2024. Urban morphology and surface urban heat island relationship during heat waves: A study of Milan and Lecce (Italy). *Remote Sensing*, 16(23), p. 4496. [DOI]

Feizizadeh, B. and Blaschke, T., 2013. Examining urban heat island relations to land use and air pollution: Multiple endmember spectral mixture analysis for thermal remote sensing. *IEEE Journal of Selected Topics in Applied Earth Observations and Remote Sensing*, 6(3), pp. 1749–1756. [DOI]

Flores, J.L., Pereira Filho, A.J. and Karam, H.A., 2016. Estimation of long term low resolution surface urban heat island intensities for tropical cities using MODIS remote sensing data. *Urban Climate*. [Preprint]. [DOI]

Fung, K.Y., Tam, C.-Y., Lee, T.-C. and Wang, Z., 2021. Comparing the Influence of Global Warming and Urban Anthropogenic Heat on Extreme Precipitation in Urbanized Pearl River Delta Area Based on Dynamical Downscaling. *Journal of Geophysical Research: Atmospheres*, 126(21), p. e2021JD035047. [DOI]

García, D.H., 2022. Analysis of Urban Heat Island and Heat Waves Using Sentinel-3 Images: a Study of Andalusian Cities in Spain. *Earth Systems and Environment*, 6(1), pp. 199–219. [DOI]

Hardin, A.W., Liu, Y., Cao, G. and Vanos, J.K., 2018. Urban heat island intensity and spatial variability by synoptic weather type in the northeast U.S. *Urban Climate*, 24, pp. 747–762. [DOI]

Holst, C.C., Tam, C.Y. and Chan, J.C.L., 2016. Sensitivity of urban rainfall to anthropogenic heat flux: A numerical experiment. *Geophysical Research Letters*, 43(5), pp. 2240–2248. [DOI]

Hu, C., Fung, K.Y., Tam, C.Y. and Wang, Z., 2021. Urbanization Impacts on Pearl River Delta Extreme Rainfall Sensitivity to Land Cover Change Versus Anthropogenic Heat. *Earth and Space Science*, 8(3), p. e2020EA001536. [DOI]

Hurduc, A., Ermida, S.L. and Da Câmara, C.C., 2024. On the Suitability of Different Satellite Land Surface Temperature Products to Study Surface Urban Heat Islands. *Remote Sensing*, 16(20), p. 3765. [DOI]

Iungman, T., Khomenko, S., Barboza, E.P., Cirach, M., Gonçalves, K., Petrone, P., Erbertseder, T., Taubenböck, H., Chakraborty, T. and Nieuwenhuijsen, M., 2024. The impact of urban configuration types on urban heat islands, air pollution, CO_2 emissions, and mortality in Europe: a data science approach. *The Lancet Planetary Health*, 8(7), pp. e489–e505. [DOI]

Jacobs, C., Klok, L., Bruse, M., Cortesão, J., Lenzholzer, S. and Kluck, J., 2020.

Are urban water bodies really cooling? *Urban Climate*, 32, p. 100607. [DOI]

Kazemi, A., Cirella, G.T., Hedayatiaghmashhadi, A. and Gili, M., 2025. Temporal-spatial Distribution of Surface Urban Heat Island and Urban Pollution Island in an Industrial City: Seasonal Analysis. *IEEE Journal of Selected Topics in Applied Earth Observations and Remote Sensing* [Preprint]. [DOI]

Kim, Y.H. and Baik, J.J., 2005. Spatial and temporal structure of the urban heat island in Seoul. *Journal of Applied Meteorology*, 44(5). [DOI]

Kolokotroni, M., Ren, X., Davies, M. and Mavrogianni, A., 2012. London's urban heat island: Impact on current and future energy consumption in office buildings. *Energy and buildings*, *47*, pp.302-311. [DOI]

Kuang, W.H., Yang, T.R., Liu, A.L., Zhang, C., Lu, D.S. and Chi, W.F., 2017. An EcoCity model for regulating urban land cover structure and thermal environment: Taking Beijing as an example. *Science China Earth Sciences*, 60(6), pp. 1098–1109. [DOI]

Luo, J., Zhu, L. and Fu, H., 2025. A new framework for mitigating urban heat island effect from the perspective of network. *Ecological Indicators*, 170, p. 113059. [DOI]

Ma, Z., Fu, H., Wen, J. and Chen, Z., 2024. Evaluating Urban Heat Island Effects in the Southwestern Plateau of China: A Comparative Analysis of Nine Estimation Methods. *Land*, 14(1), p.37. [DOI]

Nandi, D., Sing, D., Banik, A. and Mishra, P.S., 2024. Assessing urban heat island impact and identifying vulnerability zones through Geospatial and Geo-statistical techniques. *International Journal of Conservation Science*, 15(3), pp. 1577–1592. [DOI]

Novio, R., Mariya, S., Prarikeslan, W. and Ramon, S.A., 2024. Study of Temporal Dynamics of Urban Heat Island Surface in Padang, West Sumatra, Indonesia. *Nature Environment and Pollution Technology*, *23*(2), pp.1195-1200. [DOI]

Oke, T.R., 1982. The energetic basis of the urban heat island. *Quarterly Journal of the Royal Meteorological Society*. [Preprint] [DOI]

Oke, T.R., 1987. *Boundary layer climates*, 2nd edn, London: Routledge

Oke, T.R., 1988. The urban energy balance. *Progress in Physical Geography*, 12(4), pp. 471–508. [DOI]

Ouyang, Z., Sciusco, P., Jiao, T., Feron, S., Lei, C., Li, F., John, R., Fan, P., Li, X., Williams, C.A. and Chen, G., 2022. Albedo changes caused by future urbanization contribute to global warming. *Nature Communications*, *13*(1), p.3800. [DOI]

Peng, J., Qiao, R., Wang, Q., Yu, S., Dong, J. and Yang, Z., 2024. Diversified evolutionary patterns of surface urban heat island in new expansion areas of 31 Chinese cities. *npj Urban Sustainability*, *4*(1), p.14. [DOI]

Roth, M., 2007. Review of urban climate research in (sub)tropical regions. *International Journal of Climatology*. [DOI]

Schneider, A., Friedl, M.A., McIver, D.K. and Woodcock, C.E., 2003. Mapping urban areas by fusing multiple sources of coarse resolution remotely sensed data. *Photogrammetric Engineering & Remote Sensing*, *69*(12), pp.1377-1386. [DOI]

Shahmohamadi, P., Che-Ani, A.I., Maulud, K.N.A., Tawil, N.M. and Abdullah, N.A.G., 2011. The impact of anthropogenic heat on formation of urban heat island and energy consumption balance. *Urban Studies Research*, *2011*(1), p.497524. [DOI]

Shapiro, A.D. and Liu, W., 2023. Evaluating Land Surface Temperature Trends and Explanatory Variables in the Miami Metropolitan Area from 2002–2021. *Geomatics*, 4(1), pp. 1–16. [DOI]

Soltani, A. and Sharifi, E., 2017. Daily variation of urban heat island effect and its correlations to urban greenery: A case study of Adelaide. *Frontiers of Architectural Research*, 6(4), pp. 529–538. [DOI]

Streutker, D.R., 2003. Satellite-measured growth of the urban heat island of Houston, Texas. *Remote Sensing of Environment*, 85(3), pp. 282–289. [DOI]

Suazo, J.M.A., López, C.P.M. and Bartra, O.S.M., 2019. Estimation of superficial urban heat island in the metropolitan area of Iquitos [Estimación de Isla de Calor Urbana Superficial en el Área Metropolitana de Iquitos/Perú]. *Anuário do Instituto de Geociências*, 42(1), pp. 135–145. [DOI]

Suazo, J.M.A., Rojas, J.L.F. and Karam, H.A., 2020. Isla de Calor Urbana Superficial para Tres Megaciudades en África. *Anuário do Instituto de Geociências – UFRJ* [Preprint]. [DOI]

Suthar, G., Verma, P., Yadav, S. and Rani, M., 2023. Spatiotemporal variation of air pollutants and their relationship with land surface temperature in Bengaluru, India. *Remote Sensing Applications: Society and Environment*, 32, p. 101011. [DOI]

Voogt, J.A. and Oke, T.R., 2003. Thermal remote sensing of urban climates. *Remote Sensing of Environment*, 86(3), pp. 370–384. [DOI]

Wang, Z., Xu, Y., Wang, C., Liu, T., Wang, Z., Zhang, Y. and Li, Y., 2021. The projected effects of urbanization and climate change on summer thermal environment in Guangdong-Hong Kong-Macao Greater Bay Area of China. *Urban Climate*, 37, p. 100866. [DOI]

Wan, Z., 1999. *MODIS Land-Surface Temperature Algorithm Theoretical Basis Document (LST ATBD)*. Institute for Computational Earth System Science, University of California, Santa Barbara.

Wan, Z. and Li, Z.L., 1997. A physics-based algorithm for retrieving land-surface emissivity and temperature from EOS/MODIS data. *IEEE Transactions on Geoscience and Remote Sensing*, 35(4), pp. 980–996. [DOI]

Wu, X., Zhang, L. and Zang, S., 2019. Examining seasonal effect of urban heat island in a coastal city. *PLOS ONE*, 14(6), p. e0217850. [DOI]

Yao, R., Cao, J., Wang, L., Zhang, W., Chen, W. and Li, J., 2018. The influence of different data and method on estimating the surface urban heat island intensity. *Ecological Indicators*, 89, pp. 45–55. [DOI]

You, M., Zhang, H., Li, Y., Huang, Y. and Zhu, J., 2021. Quantitative analysis of a spatial distribution and driving factors of the urban heat island effect: A case study of Fuzhou central area, China. *International Journal of Environmental Research and Public Health*, 18(24), p. 13088. [DOI]

Zargari, M., Moazenzadeh, R., Raziei, T. and Sharifi, E., 2024. Climatic comparison of surface urban heat island using satellite remote sensing in Tehran and suburbs. *Scientific Reports*, 14(1), pp. 1–23. [DOI]